Original article

Title: Mechanisms of preferential bone formation in myeloma bone lesions by proteasome inhibitors

Authors: Emiko Nakaue[1], Jumpei Teramachi[2*], Hirofumi Tenshin[1], Masahiro Hiasa[1], Takeshi Harada[3], Asuka Oda[3], Yusuke Inoue[3], So Shimizu[1], Yoshiki Higa[1], Kimiko Sogabe[3], Masahiro Oura[3], Tomoyo Hara[3], Ryohei Sumitani[3], Tomoko Maruhashi[3], Hiroki Yamagami[3], Itsuro Endo[4], Eiji Tanaka[1], Masahiro Abe[3*]

Affiliations:

1. Department of Orthodontics and Dentofacial Orthopedics, Tokushima University Graduate School of Biomedical Sciences, Tokushima, Japan
2. Department of Oral Function and Anatomy, Graduate School of Medicine Dentistry and Pharmaceutical Sciences, Okayama University, Japan
3. Department of Hematology, Endocrinology and Metabolism, Tokushima University Graduate School of Biomedical Sciences, Tokushima, Japan
4. Department of Bioregulatory Sciences, Tokushima University Graduate School of Biomedical Sciences, Tokushima, Japan

Running head: Preferential bone formation by PIs (34/45 keystrokes)

Keywords: osteoblast, osteoclast, proteasome inhibitor, pulsatile treatment, multiple myeloma,

*Correspondence:
Masahiro Abe, Department of Hematology, Endocrinology and Metabolism, Tokushima University Graduate School, 3-18-15 Kuramoto, Tokushima, 770-8503, Japan, TEL.: +81-88-633-7120, FAX: +81-88-633-7121, E-mail: masabe@tokushima-u.ac.jp
Jumpei Teramachi, Department of Oral Function and Anatomy, Graduate School of Medicine Dentistry and Pharmaceutical Sciences, Okayama University Graduate School, 2-5-1 Shikata, Okayama, 700-8525, Japan, TEL.: +81-086-235-6636, FAX.: +81-235-6636, E-mail: jumptera@okayama-u.ac.jp

Word counts: Text, 6,130; Introduction to Discussion inclusive: 3,571; Abstract, 194

35 Figures/tables: Five figures.

36 References: 40 citations.

Abstract

Proteasome inhibitors (PIs) can preferentially restore bone in bone-defective lesions of patients with multiple myeloma (MM) who respond favorably to these drugs. Most prior in vitro studies on PIs used continuous exposure to low PI concentrations, although pharmacokinetic analysis in patients has shown that serum concentrations of PIs change in a pulsatile manner. In the present study, we explored the effects of pulsatile treatment with PIs on bone metabolism to simulate in vivo PI pharmacokinetics. Pulsatile treatment with bortezomib, carfilzomib, or ixazomib induced MM cell death but only marginally affected the viability of osteoclasts (OCs) with F-actin ring formation. Pulsatile PI treatment suppressed osteoclastogenesis in OC precursors and bone resorption by mature OCs. OCs robustly enhanced osteoblastogenesis in cocultures with OCs and MC3T3-E1 pre-osteoblastic cells, indicating OC-mediated coupling to osteoblastogenesis. Importantly, pulsatile PI treatment did not impair robust OC-mediated osteoblastogenesis. These results suggest that PIs might sufficiently reduce MM cell-derived osteoblastogenesis inhibitors to permit OC-driven bone formation coupling while suppressing OC differentiation and activity in good responders to PIs. OC-mediated coupling to osteoblastogenesis appears to be a predominant mechanism for preferential occurrence of bone regeneration at sites of osteoclastic bone destruction in good responders.

Introduction

Various novel anti-multiple myeloma (MM) agents have been developed. Nevertheless, repeated relapses and subsequent bone loss persist in patients with MM. MM cells stimulate bone resorption by enhancing osteoclastogenesis while suppressing bone formation by inhibiting osteoblastic differentiation from bone marrow stromal cells. Thus, MM causes extensive bone destruction and rapid bone loss [1-3]. In normal bone remodeling, homeostasis is tightly regulated by intercellular communication between osteoclasts (OCs) and osteoblasts (OBs) within the basic multicellular units of bone remodeling compartments [4]. OCs resorb damaged and old bone. In normal bone remodeling, OCs resorb bone and secrete coupling factors that recruit osteoblast precursors to the bone remodeling compartments, enhance osteoblastogenesis, and replace resorbed bone with new bone matrix [5]. In this manner, skeletal structure and integrity are maintained throughout life. In MM, however, this process is dysregulated. Besides MM cells enhance osteoclastic bone resorption while suppressing osteoblastic differentiation and, by extension, bone formation through factors such as soluble Wnt inhibitors that are secreted by the MM cells and are derived from their surrounding microenvironment [6-9]. In MM bone lesions, then, bone remodeling is skewed towards an increase in OC number and activity and the disruption of OC-mediated bone formation in the bone remodeling compartments.

Proteasome inhibitors (PIs) are major backbone drugs in MM treatment [10]. Proteasomes control the equilibrium between protein synthesis and degradation and maintain cellular function and survival. Proteasome inhibition results in the accumulation of misfolded and functional proteins ~~i~~n the lumen of the endoplasmic reticulum (ER) and the cytosol, thereby resulting in ER overload, reactive oxygen species (ROS) overproduction, functional intracellular protein disorders, and apoptosis in MM cells [11-13].

During PI treatment, bone formation is restored in the bone-destructive lesions of patients that respond favorably to these drugs [14-17]. Therefore, tumor reduction might trigger the anabolic effects of PIs by reducing MM cell-derived bone formation inhibitors. Unlike other novel anti-MM agents, PIs apparently induce robust bone formation preferentially in the bone-defective lesions that appear in radiographic images. However, the underlying mechanisms by which PIs mediate preferential bone recovery in the bone lesions of MM remain unknown.

Most prior *in vitro* studies on PIs consisted of long-term continuous exposures to low

concentrations of PIs. Nevertheless, this approach does not accurately reflect the serum pharmacokinetic profile of PIs in human patients actually being administered these drugs [18-20]. In the present study, we endeavored to simulate the *in vivo* pharmacokinetics of PIs in human patients by examining the impact of pulsatile treatment at high PI concentrations on bone metabolism. We showed that pulsatile PI treatment suppressed osteoclastogenesis in OC precursors and bone resorption by mature OCs. By contrast, pulsatile PI treatment did not reduce OC viability although it promoted MM cell death. To mimic the bone remodeling, we first prepared mature OCs *in vitro*, and then MC3T3-E1 pre-osteoblastic cells were added to coculture with mature OCs; osteoblastogenesis of MC3T3-E1 cells was robustly enhanced in the presence of OCs, indicating OC-mediated coupling to osteoblastogenesis. The robust osteoblastogenesis of MC3T3-E1 cells was similarly observed upon pulsatile PI treatment after cocultures with OCs as well as in cocultures with pulsatile PI-pretreated OCs. These results suggest that pulsatile PI treatment suppress OC differentiation and activity while retaining OC's potential to stimulate bone formation, namely OC-mediated coupling to osteoblastogenesis. OC-driven osteoblastogenesis might be a major mechanism by which bone is rebuilt in the bone-defective lesions where OCs reside in MM patients who respond rapidly and favorably to PIs. Therefore, OC-driven osteoblastogenesis, suppression of bone resorption by OCs, and the removal of osteoblastogenesis inhibitors via MM tumor reduction might cause preferential restoration of bone formation rather in osteoclastic bone destructive lesions in patients treated with PIs.

Materials and Methods

Reagents

The following reagents were purchased from the indicated manufacturers: rabbit antibodies against c-Fos, IκBα, RelA, integrin β3, Sphingosine-1-phosphate (S1P) ; horseradish peroxidase-conjugated anti-rabbit and anti-mouse IgG (Cell Signaling Technology, Beverly, MA); mouse antibody against NFATc1, ephrinB2, cadherin 11 (CDH11, OB-cadherin) (Santa Cruz Biotechnology, Dallas, TX); rabbit antibody against p84, cathepsinK, Osterix/Sp7 (Abcam, Cambridge, UK); mouse antibody against β-actin (Sigma-Aldrich, St. Louis, MO); recombinant human M-CSF, β-glycerophosphate, ascorbic acid, and bortezomib (BTZ) (Cell Signaling Technology); carfilzomib (CFZ) (Chemietek, Indianapolis, IN); MLN2238 (ixazomib) (Karebay Biochem, Monmouth Junction, NJ); recombinant human BMP-2 (R&D Systems, Minneapolis, MN); and human-soluble receptor activator of NF-κB ligand (RANKL) (Oriental Yeast, Shiga, Japan).

MM cells and cell culture

The human MM cell line MM.1S was obtained from the American Type Culture Collection (ATCC; Rockville, MD). The human MM cell line INA-6 was kindly provided by Renate Burger of the University of Kiel, Kiel, Germany. The mouse MM cell line 5TGM1 was kindly provided by Gregory R. Mundy of the Vanderbilt Center for Bone Biology, Vanderbilt University, Nashville, TN. All cells were cultured in RPMI 1640 medium (Sigma-Aldrich) supplemented with 10% (v/v) FBS and 50 mg/mL of penicillin/streptomycin (Thermo Fisher Scientific, Waltham, MA). The murine pre-osteoclastic cell line (RAW264.7) and the pre-osteoblastic cell line (MC3T3-E1) were purchased from ATCC and cultured in α-MEM (Sigma-Aldrich) supplemented with 10% (v/v) FBS and 50 mg/mL of penicillin/streptomycin.

Osteoclast (OC) differentiation

OCs were produced from the murine pre-osteoclastic cell line RAW264.7 [21] or from mouse bone marrow cells as previously described [22]. The RAW264.7 cells (2×10^4/mL) were cultured in M-CSF (10 ng/mL) and RANKL (50 ng/mL) for 4 days to generate mature OCs. Whole bone marrow cells were harvested from the femurs of C57BL/6J mice (SLC, Tokyo, Japan). Nonadherent bone marrow cells (1×10^5/mL) were collected and cultured in M-CSF (10 ng/mL) for 3 days to generate primary bone marrow-derived macrophages (BMMs) which were then cultured for 7–10 days in M-CSF (10 ng/mL) and RANKL (50 ng/mL) to generate

mature OCs. The culture medium was changed every 2 days. The cells were fixed with 10% (v/v) neutral-buffered formalin. Tartrate-resistant acid phosphatase (TRAP)-positive cells were detected with a leukocyte acid phosphatase assay kit (Wako Pure Chemical, Osaka, Japan). TRAP-positive cells were observed under a light microscope (BZ-X800; Keyence, Osaka, Japan). Those containing ≥ 3 nuclei were scored as OCs. To investigate the effects of proteasome inhibitors (PIs) on osteoclastogenesis, primary BMMs and RAW264.7 cells were either untreated or subjected to BTZ (200 nM) or CFZ (500 nM) for 1 hour or MLN2238 (200 nM) for 4 hours. After the pulsatile PI treatment, the cells were washed twice with phosphate-buffered saline (PBS) and then cultured with M-CSF (10 ng/mL) and RANKL (50 ng/mL) for 4-7 days. OC differentiation was assessed by enumerating the multinucleate TRAP-positive cells. All mouse experiments were performed under the regulation and with the permission of the Animal Care and Use Committee of the Tokushima University, Tokushima, Japan (certificate No. T2022-13).

Cell viability

Cell viability was determined by cell counting kit-8 (CCK-8) assay (Dojindo, Kumamoto, Japan) according to the manufacturer's instructions. The MM cells, BMMs, mature primary OCs, RAW264.7 cells and MC3T3-E1 cells were cultured in 96-well plates containing BTZ (200 nM) or CFZ (500 nM) for 1 hour, MLN2238 (200 nM) for 4 hours. The absorbance of each well was measured at 450–655 nm in an iMark microplate reader (Bio-Rad Laboratories, Hercules, CA).

Bone resorption assay

The effect of the PIs on RANKL-induced bone resorption was analyzed with a bone resorption assay kit in 48-well plates coated with fluorescein-labeled calcium phosphate (PG Research, Tokyo, Japan) as previously described [23]. Equal numbers of OCs generated from primary BMMs were seeded onto the assay plates and cultured with M-CSF (10 ng/mL) and RANKL (50 ng/mL) overnight. The OCs were treated with BTZ (200 nM) or CFZ (500 nM) for 1 hour, MLN2238 (200 nM) for 4 hours. The cells were then washed with PBS and further cultured in phenol red free α-MEM with M-CSF (10 ng/mL) and RANKL (100 ng/mL) for 48 hours. The culture supernatants were collected, and calcium phosphate fluorescence intensity was measured in a microplate reader (SpectraMax i3; Molecular Devices, LLC, San Jose, CA). Bone resorption activity was determined by measuring the resorbed area with ImageJ software (National Institutes of Health, Bethesda, MD; http://imagej.nih.gov/ij/).

F-actin ring staining

RAW264.7 cells were cultured in RANKL (50 ng/mL) to generate mature OCs which were then treated with BTZ (200 nM) or CFZ (500 nM) for 1 hour, MLN2238 (200 nM) for 4 hours. They were washed with PBS and cultured in RANKL (50 ng/mL) for 24 hours. The OCs were fixed and stained with Acti-stain^{TM} 488 phalloidin (Cytoskeleton, Denver, CO) following the manufacturer's instructions and observed under a fluorescence microscope (BZ-X800; Keyence). DAPI (Thermo Fisher Scientific) was used to stain the nuclei of cells.

OB differentiation

MC3T3-E1 cells were cultured in osteoblastic media (10 ng/mL BMP-2, 10 mM β-glycerophosphate, and 50 μg/mL ascorbic acid in 10% (v/v) FBS containing α-MEM). To examine OB differentiation, the cells were fixed with 10% (v/v) neutral-buffered formalin and visualized with an alkaline phosphatase staining kit (Wako Pure Chemical). The scanned images were analyzed with ImageJ software to measure the alkaline phosphatase (ALP)-positive areas.

Co-culture experiments

Two types of experiments with pulsatile PI treatment were performed as follows: 1) Primary mature OCs prepared culture wells were first treated with or without BTZ (200 nM) or CFZ (500 nM) for 1 hour or MLN2238 (200 nM) for 4 hours. They were then washed twice with PBS, and MC3T3-E1 cells (1×10^5/well) were seeded and cocultured with the OCs in osteoblastic media for 2 days. 2) MC3T3-E1 cells were first seeded onto primary mature OCs and both were treated with or without BTZ (200 nM) or CFZ (500 nM) for 1 hour or MLN2238 (200 nM) for 4 hours. The cells were then washed with PBS, and then cultured in osteoblastic media for 2 days. OB differentiation was assessed by ALP staining.

Western blot analysis

Cells were collected and digested in RIPA lysis buffer (Santa Cruz Biotechnology). For cytosolic and nuclear preparation, the cells were lysed in NE-PER extraction reagent (Thermo Fisher Scientific) according to the manufacturer's instructions. Western blot analysis was done with equal protein amounts of cell lysate, as described previously [24].

Statistical analysis

211 Pairwise data comparisons were made with Student's *t*-test. For multiple comparisons,
212 statistical differences were determined by one-way analysis of variance (ANOVA) followed by
213 Tukey's test. $P < 0.05$ indicated a significant difference. All statistical analyses were performed
214 with Statcel v. 4 software (OMS Publishing, Saitama, Japan).

Results

Proteasome inhibitor (PI) pulse treatment induced cell death in MMs but not OCs

Pharmacokinetic profiles of human patients treated with PIs disclosed that their serum PI concentrations reached C_{max} > 1 μM immediately after administration, rapidly declined to nanomolar levels, and remained there for 1 week [18-20]. Hence, we applied 200 nM BTZ and 500 nM CFZ for 1 hour and 200 nM MLN2238 for 4 hours to simulate the pharmacodynamics and pharmacokinetics of these drugs in human patients.

We assessed the effects of pulsatile PI treatment on cell viability. Pulsatile treatment with the PIs BTZ, CFZ, and MLN2238 did not reduce the viability of bone marrow macrophages (BMMs), mature OCs, RAW264.7 preosteoclastic cell line or MC3T3-E1 pre-osteoblastic cell line (Figure 1a). By contrast, pulsatile treatment with these PIs at the same concentrations induced cell death in the MM cell lines MM.1S, INA-6 and 5TGM1 (Figure 1b). We further evaluated the direct effects of pulsatile PI treatment on mature OCs. F-actin ring formation and integrin β3 expression are vital to mature OC viability and activity. Large F-actin rings are characteristic of mature OCs and they appeared in the control cultures (Figure 2a). After the pulsatile PI treatment, F-actin ring formation persisted in the large OCs. Integrin β3 was expressed in the mature OCs but did not decrease after the pulsatile PI treatment (Figure 2b). Cathepsin K is a specific marker of mature OCs. PI pulse treatment did not affect cathepsin K expression in mature OCs (Figure 2c). The preceding results suggest that OCs but not MM cells resist pulsatile PI treatment.

Pulsatile PI treatment suppressed RANKL-mediated osteoclastogenesis

RANKL is a critical osteoclastogenesis mediator and is aberrantly upregulated to enhance osteoclastogenesis and bone resorption in MM bone lesions. We explored the effect of the pulsatile PI treatment on OC differentiation. M-CSF and soluble RANKL addition induced TRAP-positive multinucleated cell formation. That is, BMMs (Figure 3a) and RAW264.7 pre-osteoclastic cells (Figure 3b) differentiated into OCs. However, the pulsatile PI treatment suppressed TRAP-positive multinucleated cell formation from BMMs and RAW264.7 cells. NFATc1 and c-Fos are critical transcription factors (TFs) in osteoclastogenesis and were upregulated in the RAW264.7 cells subjected to RANKL (Figure 3c). The pulsatile PI treatment abolished NFATc1 and c-Fos upregulation. RANKL-induced activation of the NF-κB signaling pathway is vital for osteoclastogenesis. RANKL treatment promoted IκBα degradation (Figure

3d), and nuclear localization of RelA, the NF-κB subunit p65, (Figure 3e) in RAW264.7 cells. The pulsatile treatment with PIs abrogated these RANKL-induced changes. Therefore, the pulsatile PI treatment might suppress RANKL-induced osteoclastogenesis in part by inhibiting the NF-κB signaling pathway.

Pulsatile PI treatment suppressed OC bone resorption capacity

Mature OCs were spared from cell death by the pulsatile PI treatment (Figure 1). Nevertheless, we examined OC function after this treatment. OCs were prepared from BMMs, harvested, and plated on fluoresceinated calcium phosphate-coated dishes. Bone resorption activity was estimated from the pits formed in the fluoresceinated calcium phosphate-coated plates. Supernatant fluorescence intensity in the presence or absence of pulsatile PI treatment was evaluated. The pulsatile PI treatment reduced the relative supernatant fluorescence intensity, the relative number of pits and pit areas formed by the OCs (Figure 4a). The representative images of the pit formation were shown in Figure 4b. Thus, the pulsatile PI treatment suppressed bone resorptive activity without impairing OC's viability.

Pulsatile PI treatment preserved robust OC-mediated osteoblastogenesis

OCs induce bone formation at bone resorption sites through OC-derived coupling to osteoblastogenesis. This mechanism depends on the communication between OCs and osteoblasts. We examined OC-derived osteoblastogenesis coupling in response to the pulsatile PI treatment in osteogenic MC3T3-E1 pre-osteoblastic cell cultures. When the MC3T3-E1 pre-osteoblastic cells were cultured alone or plated and co-cultured with the OCs prepared in the culture wells, the OC co-cultured with MC3T3-E1 cells presented substantially enhanced alkaline phosphatase (ALP) activity, an indicator of early osteoblastogenesis. The enhancement of osteoblastogenesis by OCs was maintained either in MC3T3-E1 cells co-cultured with OCs pretreated with the pulsatile treatment with PIs (Figure 5a) or in both MC3T3-E1 cells and OCs exposed to pulsatile PI treatment after co-culture (Figure 5b). Osterix is an essential transcription factor for osteoblastogenesis and regarded as a good marker for osteoblastic differentiation. Osterix was upregulated in MC3T3-E1 cells in co-cultured with OCs; however, the pulsatile PIs did not affect the OC-mediated induction of osterix in MC3T3-E1 cells (Figure 5c). OCs may produce several coupling factors including ephrinB2 and sphingosine-1-phosphate (S1P) which can trigger osteoblastogenesis [25, 26]. Both ephrin B2 and S1P remained upregulated in the OCs following the pulsatile PI treatment (Figure 5d). These results demonstrate that OCs can potently induce osteoblastogenesis and suggest that pulsatile PI

283 treatment maintains OC-derived coupling to osteoblastogenesis while suppressing OC's bone
284 resorption activity and inducing MM cell death.

Discussion

In clinical practice, patients treated with PIs achieve a good response with very good partial response or more have been demonstrated to resume significant bone formation preferentially in osteoclastic bone destructive MM lesions without hyperostosis in normal bones, which is a therapeutic merit unique to PIs [14-17] . Patients with MM exhibiting bone formation tend to show a better and prolonged reduction of MM tumor. PIs have been demonstrated to transcriptionally upregulate Runx2 [27, 28] which is a critical TF in early osteoblastogenesis and cause the accumulation of various mediators of the β-catinine, Osterix/Sp7, and ATF4 signaling pathways responsible for osteoblastogenesis by blockading their proteasomal degradation [29, 17, 30]. PIs also suppressed DKK1 production in the bone marrow microenvironment and sclerostin production in osteocytes [17, 31] . Bortezomib can protect bone loss in non-tumorous animal osteoporotic models [28, 32]. With enough reduction of MM tumor cells, PIs are thought to enhance the levels of critical osteoblastogenesis-related TFs such as Runx2 and ATF4 [27, 30], and thereby rebuild bone in MM. The direct effects of PIs on osteoblastogenesis have been demonstrated mainly by *in vitro* cultures of osteoblastic lineage cells with long-term exposure to relatively low concentrations of PIs. Continuous treatment with PIs at higher concentrations (ex. Bortezomib over 10 nM) rather hampered *in vitro* osteoblastogenesis [30]. However, MM patients treated with PIs exhibit pulsatile high PI concentrations in their sera. Only with the direct anabolic actions of PIs, it is hard to explain rapid and selective bone recovery in bone-defective lesions without hyperostosis in normal bones in good responders to PIs.

In terms of the experimental conditions of bortezomib or carfilzomib exposure, we basically followed the previous paper with experiments modeling the anticipated *in vivo* pharmacokinetics of drug exposure in which MM cells were treated with pulsatile treatment for one hour of bortezomib or carfilzomib at concentrations mainly between 100 and 300 and between 100 and 500 nM, respectively [33]. However, carfilzomib can be currently used with 30-minute iv infusion at 70 mg/m² which makes much higher maximum observed plasma concentrations (Cmax) compared with those with the administration at 27 and 56 mg/m². Therefore, we set experimental conditions with one-hour treatment of carfilzomib at 500 nM, the highest concentration in the previous paper [33]. Ixazomib is an oral agent and thus its inter-patient variability in Cmax is wide. Maximum drug concentration time from oral intake (Tmax) was also widely distributed over 3 hours. Therefore, blood concentrations of ixazomib can reach 200 nM for 4 hours in a certain portion of patients after taking ixazomib orally. By taking into

consideration the wide distribution of Cmax and Tmax with long T1/2, we set 200 nM for 4 hours as an experimental condition for MLN2238 exposure to mimic a PK profile in patients with good bioavailability of this drug. Here, we examined the effects of short-term pulsatile treatment with BTZ (200 nM) and CFZ (500 nM) for 1 hour and MLN2238 (200 nM) for 4 hours to simulate the pharmacokinetic profile of PIs in MM patients treated with them. The pulsatile PI treatment suppressed the osteoclastogenesis of OC precursors and bone resorption by mature OCs without impairing OC viability. We previously reported that OCs and their precursors resisted the ROS-inducible anti-cancer agent doxorubicin and utilized ROS in their own differentiation and activation [34]. Doxorubicin enhanced RANKL-induced osteoclastogenesis by inducing NFATc1 which is a critical TF in early osteoclastogenesis. The results of the present study suggested that OCs and their precursors resist pulsatile PI treatment at high concentrations as the cells maintained their viability and F-actin ring formation. By contrast, MM cells underwent cell death under the same treatments. Unlike doxorubicin, however, the pulsatile PI treatment suppressed RANKL-induced NFATc1 expression and thereby osteoclastic differentiation, and repressed bone resorption by mature OCs.

After OCs resorb damaged or old bone during normal bone remodeling, they locally produce multiple coupling factors, enhance osteoblastogenesis, and replace the resorbed bone with new bone matrix [5]. Thus, OCs are vital for potent osteogenic activity and effective bone formation. Here, osteoblastogenesis was markedly induced in the presence of OCs (Figure 5). Hence, there was a coupling between OCs and osteoblasts resulting in OC-induced osteoblastogenesis or bone formation. Robust OC-induced osteoblastogenesis persisted in response to the pulsatile PI treatment. MM cells overproduce inhibitory factors for osteoblastogenesis including the soluble Wnt antagonists DKK1 and sFRP family members, and we previously reported that MM cell-derived conditioned media suppress osteoblastogenesis [7][35]. In active MM bone lesions where MM cells and OCs accumulate, osteoblastogenesis is markedly suppressed. However, substantial MM cell reduction with PIs allows OC-mediated osteoblastogenesis through elimination of the MM cell-derived inhibitors. Therefore, OC-driven osteoblastogenesis might be the predominant mechanism by which bone is restored in bone-defective lesions where OCs reside under PI-based treatment. In patients who respond favorably to PIs, PIs may sufficiently reduce MM cell-derived inhibitors for osteoblastogenesis to facilitate OC-driven bone formation coupling and the suppression of OC differentiation and activity.

Suppression of OC's bone resorptive activity with retaining OC viability has been demonstrated

to efficiently increase bone formation in patients with osteoporosis under treatment with cathepsin K inhibitors [36]. Cathepsin K inhibitors inhibit the enzymatic degradation of bone matrix by cathepsin K secreted from mature active OCs without affecting OC viability. Although cathepsin K inhibitors do not directly affect osteoblastogenesis, treatment with cathepsin K inhibitors has been demonstrated to robustly enhance bone formation [37, 38]. Cathepsin K inhibition might permit OCs to enhance osteoblastogenesis by inducing coupling factor production by OCs while suppressing OC bone resorption [39]. As observed in a randomized, double-blind, multicenter phase 3 study of denosumab compared with zoledronic acid in the treatment of bone disease in subjects with newly diagnosed MM with at least one image-documented bone lesion, 60% of new skeletal related events on study occurred within the first 3 months [40], suggesting the presence of active OCs after administration of these potent anti-bone resorptive agents. Thus, abundant active OCs persist in osteoclastic bone lesions in the early course of anti-MM treatment under repeated denosumab or zoledronic acid administration. By analogy with the anabolic effects of cathepsin K inhibitors, the pulsatile PI treatment suppressed bone resorption by mature OCs in MM bone lesions while permitting viable OCs to couple to osteoblastogenesis in early responders with substantially reducing MM cell-derived inhibitors for osteoblastogenesis. Taken together, the mechanistic view of OC-driven coupling to osteoblastogenesis explains why bone regeneration preferentially occurs in bone-destructive lesions in good responders during the early course of PI-based treatment.

Acknowledgements

This work was supported in part by JSPS KAKENHI Grants Nos. JP17KK0169, JP21H03111, and JP22K19626 to J.T., JP22H03104 to M.A., JP20K18784 to H.T., and JP22K08455 to T.H., a Japanese Society of Hematology Research Grant (No. 20247 to J.T.), a Research Clusters Program of Tokushima University Grant (No. 1803003 to M.A.), and a Research Clusters Program of Tokushima University Grant (No. 2202003 to T.H.). The funders had no role in the study design, data collection and analysis, decision to publish, or manuscript preparation.

Authorship

E.N., J.T., H.T., and M.A. designed the research and conceived the project. E.N., J.T., H.T., M.O., H.Y., and R.S. conducted the *in vitro* cultures. E.N., J.T., H.T., T.H., A.O., Y.I., and S.S. performed the western blots. E.N., J.T., M.H., Y.H., K.S. and H.T. conducted the immunofluorescence assays. E.N., J.T., H.T., T.H., and T.M. analyzed the data. I.E., E.T., and M.A. supervised the project. E.N., J.T., H.T., and M.A. wrote the original draft. All authors consented to the final submitted draft version of the manuscript.

Conflict of interest

M.A. received research funding from Chuagai Pharmaceutical, Sanofi K.K., Kyowa Kirin, Janssen Pharmaceutical K.K., Takeda Pharmaceutical, Teijin Pharma, and Ono Pharmaceutical, and honoraria from Daiichi Sankyo Co. All other authors have no competing financial interests to declare.

References

1. Raje N, Roodman GD. Advances in the biology and treatment of bone disease in multiple myeloma. Clin Cancer Res. 2011;17(6):1278-86. doi:10.1158/1078-0432.Ccr-10-1804.
2. Hiasa M, Harada T, Tanaka E, Abe M. Pathogenesis and treatment of multiple myeloma bone disease. Jpn Dent Sci Rev. 2021;57:164-73. doi:10.1016/j.jdsr.2021.08.006.
3. Harada T, Hiasa M, Teramachi J, Abe M. Myeloma-Bone Interaction: A Vicious Cycle via TAK1-PIM2 Signaling. Cancers (Basel). 2021;13(17). doi:10.3390/cancers13174441.
4. Matsuo K, Irie N. Osteoclast-osteoblast communication. Arch Biochem Biophys. 2008;473(2):201-9. doi:10.1016/j.abb.2008.03.027.
5. Durdan MM, Azaria RD, Weivoda MM. Novel insights into the coupling of osteoclasts and resorption to bone formation. Semin Cell Dev Biol. 2022;123:4-13. doi:10.1016/j.semcdb.2021.10.008.
6. Tian E, Zhan F, Walker R, Rasmussen E, Ma Y, Barlogie B et al. The role of the Wnt-signaling antagonist DKK1 in the development of osteolytic lesions in multiple myeloma. N Engl J Med. 2003;349(26):2483-94. doi:10.1056/NEJMoa030847.
7. Oshima T, Abe M, Asano J, Hara T, Kitazoe K, Sekimoto E et al. Myeloma cells suppress bone formation by secreting a soluble Wnt inhibitor, sFRP-2. Blood. 2005;106(9):3160-5. doi:10.1182/blood-2004-12-4940.
8. Heath DJ, Chantry AD, Buckle CH, Coulton L, Shaughnessy JD, Jr., Evans HR et al. Inhibiting Dickkopf-1 (Dkk1) removes suppression of bone formation and prevents the development of osteolytic bone disease in multiple myeloma. J Bone Miner Res. 2009;24(3):425-36. doi:10.1359/jbmr.081104.
9. McDonald MM, Reagan MR, Youlten SE, Mohanty ST, Seckinger A, Terry RL et al. Inhibiting the osteocyte-specific protein sclerostin increases bone mass and fracture resistance in multiple myeloma. Blood. 2017;129(26):3452-64. doi:10.1182/blood-2017-03-773341.
10. Anderson KC. The 39th David A. Karnofsky Lecture: bench-to-bedside translation of targeted therapies in multiple myeloma. J Clin Oncol. 2012;30(4):445-52. doi:10.1200/jco.2011.37.8919.
11. Adams J. The proteasome: a suitable antineoplastic target. Nat Rev Cancer. 2004;4(5):349-60. doi:10.1038/nrc1361.
12. Pérez-Galán P, Roué G, Villamor N, Montserrat E, Campo E, Colomer D. The proteasome inhibitor bortezomib induces apoptosis in mantle-cell lymphoma through generation of ROS and Noxa activation independent of p53 status. Blood. 2006;107(1):257-64. doi:10.1182/blood-2005-05-2091.
13. Fink EE, Mannava S, Bagati A, Bianchi-Smiraglia A, Nair JR, Moparthy K et al. Mitochondrial thioredoxin reductase regulates major cytotoxicity pathways of proteasome inhibitors in multiple myeloma cells. Leukemia. 2016;30(1):104-11. doi:10.1038/leu.2015.190.
14. Zangari M, Esseltine D, Lee CK, Barlogie B, Elice F, Burns MJ et al. Response to bortezomib is associated to osteoblastic activation in patients with multiple myeloma. Br J Haematol. 2005;131(1):71-3. doi:10.1111/j.1365-2141.2005.05733.x.
15. Ozaki S, Tanaka O, Fujii S, Shigekiyo Y, Miki H, Choraku M et al. Therapy with bortezomib plus dexamethasone induces osteoblast activation in responsive patients with multiple myeloma. Int J Hematol. 2007;86(2):180-5. doi:10.1532/ijh97.07030.
16. Zangari M, Aujay M, Zhan F, Hetherington KL, Berno T, Vij R et al. Alkaline phosphatase variation during carfilzomib treatment is associated with best response in multiple myeloma patients. Eur J Haematol. 2011;86(6):484-7. doi:10.1111/j.1600-0609.2011.01602.x.
17. Zangari M, Suva LJ. The effects of proteasome inhibitors on bone remodeling in multiple myeloma. Bone. 2016;86:131-8. doi:10.1016/j.bone.2016.02.019.
18. Moreau P, Coiteux V, Hulin C, Leleu X, van de Velde H, Acharya M et al. Prospective comparison of subcutaneous versus intravenous administration of bortezomib in patients with

multiple myeloma. Haematologica. 2008;93(12):1908-11. doi:10.3324/haematol.13285.
19. O'Connor OA, Stewart AK, Vallone M, Molineaux CJ, Kunkel LA, Gerecitano JF et al. A phase 1 dose escalation study of the safety and pharmacokinetics of the novel proteasome inhibitor carfilzomib (PR-171) in patients with hematologic malignancies. Clin Cancer Res. 2009;15(22):7085-91. doi:10.1158/1078-0432.Ccr-09-0822.
20. Assouline SE, Chang J, Cheson BD, Rifkin R, Hamburg S, Reyes R et al. Phase 1 dose-escalation study of IV ixazomib, an investigational proteasome inhibitor, in patients with relapsed/refractory lymphoma. Blood Cancer J. 2014;4(10):e251. doi:10.1038/bcj.2014.71.
21. Teramachi J, Hiasa M, Oda A, Harada T, Nakamura S, Amachi R et al. Pim-2 is a critical target for treatment of osteoclastogenesis enhanced in myeloma. Br J Haematol. 2018;180(4):581-5. doi:10.1111/bjh.14388.
22. Shinohara H, Teramachi J, Okamura H, Yang D, Nagata T, Haneji T. Double Stranded RNA-Dependent Protein Kinase is Necessary for TNF-α-Induced Osteoclast Formation In Vitro and In Vivo. J Cell Biochem. 2015;116(9):1957-67. doi:10.1002/jcb.25151.
23. Watahiki A, Hoshikawa S, Chiba M, Egusa H, Fukumoto S, Inuzuka H. Deficiency of Lipin2 Results in Enhanced NF-κB Signaling and Osteoclast Formation in RAW-D Murine Macrophages. Int J Mol Sci. 2021;22(6). doi:10.3390/ijms22062893.
24. Teramachi J, Tenshin H, Hiasa M, Oda A, Bat-Erdene A, Harada T et al. TAK1 is a pivotal therapeutic target for tumor progression and bone destruction in myeloma. Haematologica. 2021;106(5):1401-13. doi:10.3324/haematol.2019.234476.
25. Zhao C, Irie N, Takada Y, Shimoda K, Miyamoto T, Nishiwaki T et al. Bidirectional ephrinB2-EphB4 signaling controls bone homeostasis. Cell Metab. 2006;4(2):111-21. doi:10.1016/j.cmet.2006.05.012.
26. Pederson L, Ruan M, Westendorf JJ, Khosla S, Oursler MJ. Regulation of bone formation by osteoclasts involves Wnt/BMP signaling and the chemokine sphingosine-1-phosphate. Proc Natl Acad Sci U S A. 2008;105(52):20764-9. doi:10.1073/pnas.0805133106.
27. Giuliani N, Morandi F, Tagliaferri S, Lazzaretti M, Bonomini S, Crugnola M et al. The proteasome inhibitor bortezomib affects osteoblast differentiation in vitro and in vivo in multiple myeloma patients. Blood. 2007;110(1):334-8. doi:10.1182/blood-2006-11-059188.
28. Mukherjee S, Raje N, Schoonmaker JA, Liu JC, Hideshima T, Wein MN et al. Pharmacologic targeting of a stem/progenitor population in vivo is associated with enhanced bone regeneration in mice. J Clin Invest. 2008;118(2):491-504. doi:10.1172/jci33102.
29. Qiang YW, Hu B, Chen Y, Zhong Y, Shi B, Barlogie B et al. Bortezomib induces osteoblast differentiation via Wnt-independent activation of beta-catenin/TCF signaling. Blood. 2009;113(18):4319-30. doi:10.1182/blood-2008-08-174300.
30. Nakamura S, Miki H, Kido S, Nakano A, Hiasa M, Oda A et al. Activating transcription factor 4, an ER stress mediator, is required for, but excessive ER stress suppresses osteoblastogenesis by bortezomib. Int J Hematol. 2013;98(1):66-73. doi:10.1007/s12185-013-1367-z.
31. Eda H, Santo L, Wein MN, Hu DZ, Cirstea DD, Nemani N et al. Regulation of Sclerostin Expression in Multiple Myeloma by Dkk-1: A Potential Therapeutic Strategy for Myeloma Bone Disease. J Bone Miner Res. 2016;31(6):1225-34. doi:10.1002/jbmr.2789.
32. Fang Y, Liu Y, Zhao Z, Lu Y, Shen X, Zhu T et al. Bortezomib Rescues Ovariectomy-Induced Bone Loss via SMURF-Mediated Ubiquitination Pathway. Oxid Med Cell Longev. 2021;2021:9661200. doi:10.1155/2021/9661200.
33. Kuhn DJ, Chen Q, Voorhees PM, Strader JS, Shenk KD, Sun CM et al. Potent activity of carfilzomib, a novel, irreversible inhibitor of the ubiquitin-proteasome pathway, against preclinical models of multiple myeloma. Blood. 2007;110(9):3281-90. doi:10.1182/blood-2007-01-065888.
34. Ashtar M, Tenshin H, Teramachi J, Bat-Erdene A, Hiasa M, Oda A et al. The Roles of ROS

493 Generation in RANKL-Induced Osteoclastogenesis: Suppressive Effects of Febuxostat.
494 Cancers (Basel). 2020;12(4). doi:10.3390/cancers12040929.
495 35. Hiasa M, Teramachi J, Oda A, Amachi R, Harada T, Nakamura S et al. Pim-2 kinase is an
496 important target of treatment for tumor progression and bone loss in myeloma. Leukemia.
497 2015;29(1):207-17. doi:10.1038/leu.2014.147.
498 36. Langdahl B, Binkley N, Bone H, Gilchrist N, Resch H, Rodriguez Portales J et al.
499 Odanacatib in the treatment of postmenopausal women with low bone mineral density: five
500 years of continued therapy in a phase 2 study. J Bone Miner Res. 2012;27(11):2251-8.
501 doi:10.1002/jbmr.1695.
502 37. Duong le T, Leung AT, Langdahl B. Cathepsin K Inhibition: A New Mechanism for the
503 Treatment of Osteoporosis. Calcif Tissue Int. 2016;98(4):381-97. doi:10.1007/s00223-015-
504 0051-0.
505 38. Drake MT, Clarke BL, Oursler MJ, Khosla S. Cathepsin K Inhibitors for Osteoporosis:
506 Biology, Potential Clinical Utility, and Lessons Learned. Endocr Rev. 2017;38(4):325-50.
507 doi:10.1210/er.2015-1114.
508 39. Lotinun S, Kiviranta R, Matsubara T, Alzate JA, Neff L, Lüth A et al. Osteoclast-specific
509 cathepsin K deletion stimulates S1P-dependent bone formation. J Clin Invest. 2013;123(2):666-
510 81. doi:10.1172/jci64840.
511 40. Raje N, Terpos E, Willenbacher W, Shimizu K, García-Sanz R, Durie B et al. Denosumab
512 versus zoledronic acid in bone disease treatment of newly diagnosed multiple myeloma: an
513 international, double-blind, double-dummy, randomised, controlled, phase 3 study. Lancet
514 Oncol. 2018;19(3):370-81. doi:10.1016/s1470-2045(18)30072-x.
515

Figure legends

Figure 1. Pulsatile PI treatment induced cell death in MM but not in pre-osteoblasts, bone marrow macrophages, or mature OCs

(a) Bone marrow macrophages (BMMs) and mature osteoclasts (OCs) were generated as described in the Methods section. BMMs, mature OCs, pre-osteoclastic cell line RAW264.7 and pre-osteoblastic cell line MC3T3-E1 were subjected to pulsatile PI treatment as described in the Methods section. The treated cells were washed and then cultured for 24 hours. Cell viability was determined by WST-8 assay. Data are means ± SD of six biological replicates. (b) The human MM cell lines MM.1S and INA-6 and the murine 5TGM1 MM cell line were subjected to pulsatile PI treatment as described in the Methods section. The treated cells were washed and then cultured for 24 hours. Cell viability was determined by WST-8 assay. Data are means ± SD of six biological replicates. *$p < 0.05$ by ANOVA followed by Tukey's test.

Figure 2. F-actin ring formation was maintained in the large cells subjected to PI pulse treatment

(a) Mature OCs were plated on glass bottom dishes and subjected to PIs as described in the Methods section. The cells were washed and cultured with 50 ng/mL RANKL for 24 hours. Then, the cells were fixed and stained with Phalloidin. Scale bar = 100 μm. (b) Mature OCs were subjected to pulsatile PI treatment as described in the Methods section. The cells were washed and then cultured for the indicated time periods. Cell lysates were collected and their integrin β3 protein levels were determined by western blotting. β-actin was a loading control. (c) Mature OCs were subjected to pulsatile PI treatment as described in the Methods section. The cells were washed and then cultured for the indicated time periods. Cell lysates were collected, and their cathepsin K protein levels were determined by western blotting. β-actin was a loading control.

Figure 3. Pulsatile PI treatment suppressed RANKL-induced osteoclastogenesis

BMMs (a) or RAW264.7 cells (b) were pre-treated with or without BTZ (200 nM) or CFZ (500 nM) for 1 hour, or with MLN2238 (200 nM) for 4 hours. The BMMs and RAW264.7 cells were washed and cultured with M-CSF (10 ng/mL) and RANKL (50 ng/mL) for 7 and 4 days, respectively. The cells were then fixed and stained with TRAP. TRAP-positive cells containing ≥ 3 nuclei were counted. Data are means ± SD of four biological replicates. * $p < 0.05$ by ANOVA followed by Tukey's test. Representative photographs are shown. Original magnification = ×100. Bar = 100 μm. (c) RAW264.7 cells with or without pulsatile PI

pretreatment were cultured with or without RANKL (50 ng/mL) for 24 hours. NFATc1 and c-Fos protein levels were determined by western blotting. β-actin was a loading control. (d) RAW264.7 cells with or without pulsatile PI pretreatment were cultured with RANKL (50 ng/mL) for 10 and 20 minutes. IκBα protein levels were determined by western blotting. β-actin was the loading control. (e) RAW264.7 cells with or without pulsatile PI pretreatment were cultured with RANKL (50 ng/mL) for 24 hours. Nuclear extracts were prepared and subjected to western blot analysis with anti-Rel A antibody. p84 was a loading control.

Figure 4. Pulsatile PI treatment suppressed bone resorption by mature OCs

(a) Mature OCs were applied to osteo-assay plates and subjected to PI treatment as described in the Methods section. The cells were washed and cultured in the presence of RANKL (50 ng/mL) for 2 days. The culture media were collected, and the calcium phosphate fluorescence intensity was measured (left). The total number of resorption pits (middle) were counted, and the total areas of resorption pits (right) were analyzed as described in the Methods section. Data are means ± SD of four biological replicate. *$p < 0.05$ by ANOVA followed by Tukey's test. (b) Representative photomicrographs of the bone resorption area were shown. Scale bar = 100 μm.

Figure 5. Pulsatile PI treatment retained and exerted OC-mediated bone mineralization *in vitro*

(a) Mature OCs in the indicated wells were subjected to pulsatile PI treatment as described in the Methods section. The cells were washed and MC3T3-E1 cells were superimposed on them. The two cell types were co-cultured in the osteogenic media for 2 days. OB differentiation was analyzed by ALP staining and the ALP-positive areas (mm^2) were measured. Data are means ± SD of four biological replicates. *$p < 0.05$ by ANOVA followed by Tukey's test. Photomicrographs of the ALP-positive area were shown. Scale bar = 10 mm. (b) MC3T3-E1 cells were superimposed on mature OCs and both types of cells in the indicated wells were subjected to pulsatile PI treatment as described in the Methods section. The cells were then washed and co-cultured in the osteogenic media for 2 days. OB differentiation was analyzed by ALP staining and the ALP-positive areas (mm^2) were measured. (c) Mature OCs were subjected to pulsatile PI treatment as described in the Methods section. The cells were washed and then MC3T3-E1 cells were superimposed on them and co-cultured in the osteogenic media for 2 days. Cell lysates were collected, and osterix protein levels were determined by western blotting. The osteoblast-specific protein CDH11 (OB-cadherin) was used to estimate the loaded amounts

584 of osteoblast-derived lysates. (d) Mature OCs generated from RAW264.7 pre-osteoclastic cells
585 were subjected to pulsatile PI treatment as described in the Methods section, and then washed
586 and cultured for the indicated periods. Cell lysates were collected and their ephrinB2 and S1P
587 protein levels were determined by western blotting. β-actin was a loading control.

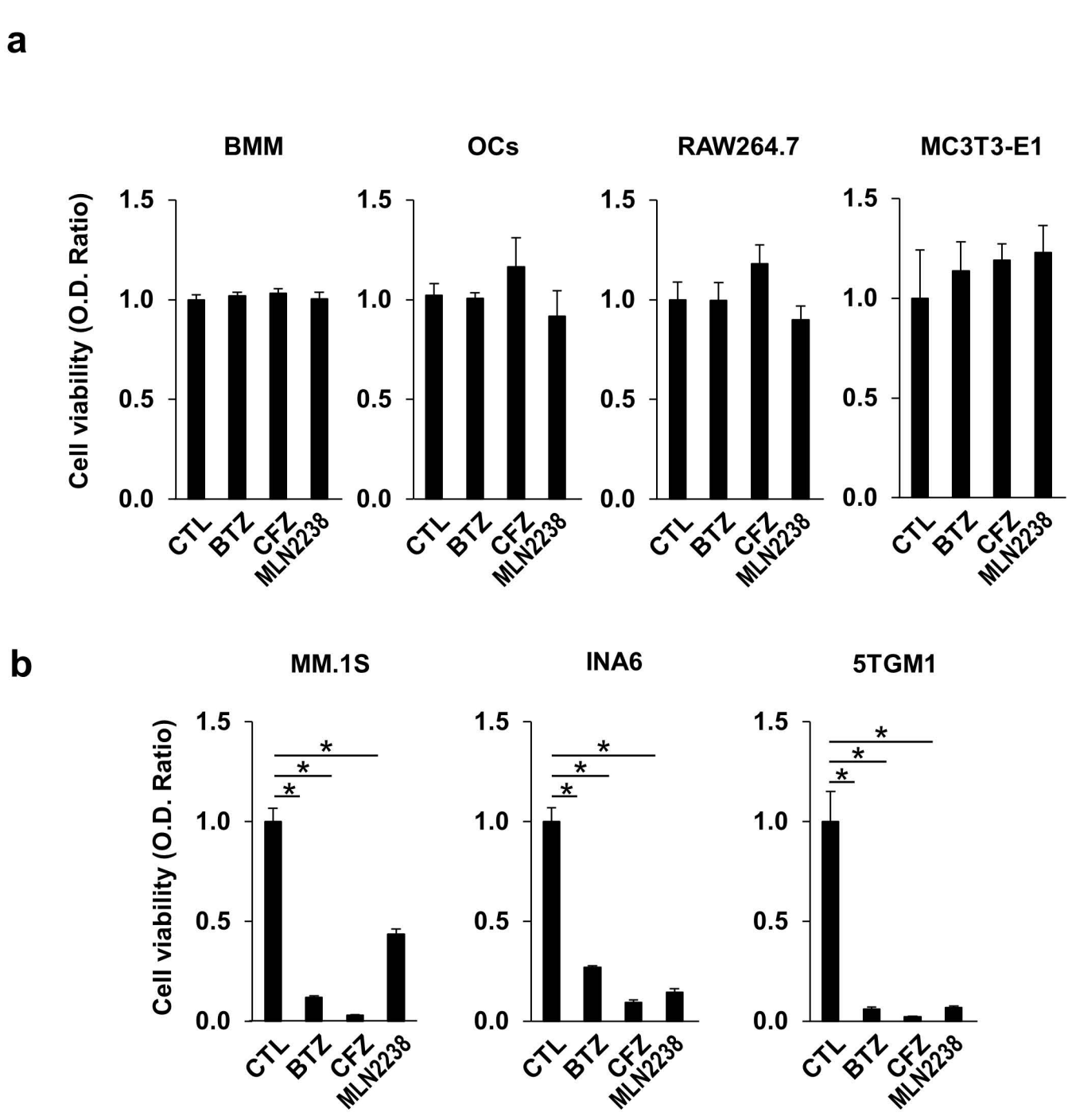
a
BMM
OCs
RAW264.7
MC3T3-E1
Cell viability (O.D. Ratio)
1.5
1.0
0.5
0.0
CTL
BTZ
CFZ
MLN2238
b
MM.1S
INA6
5TGM1
*

Figure 1

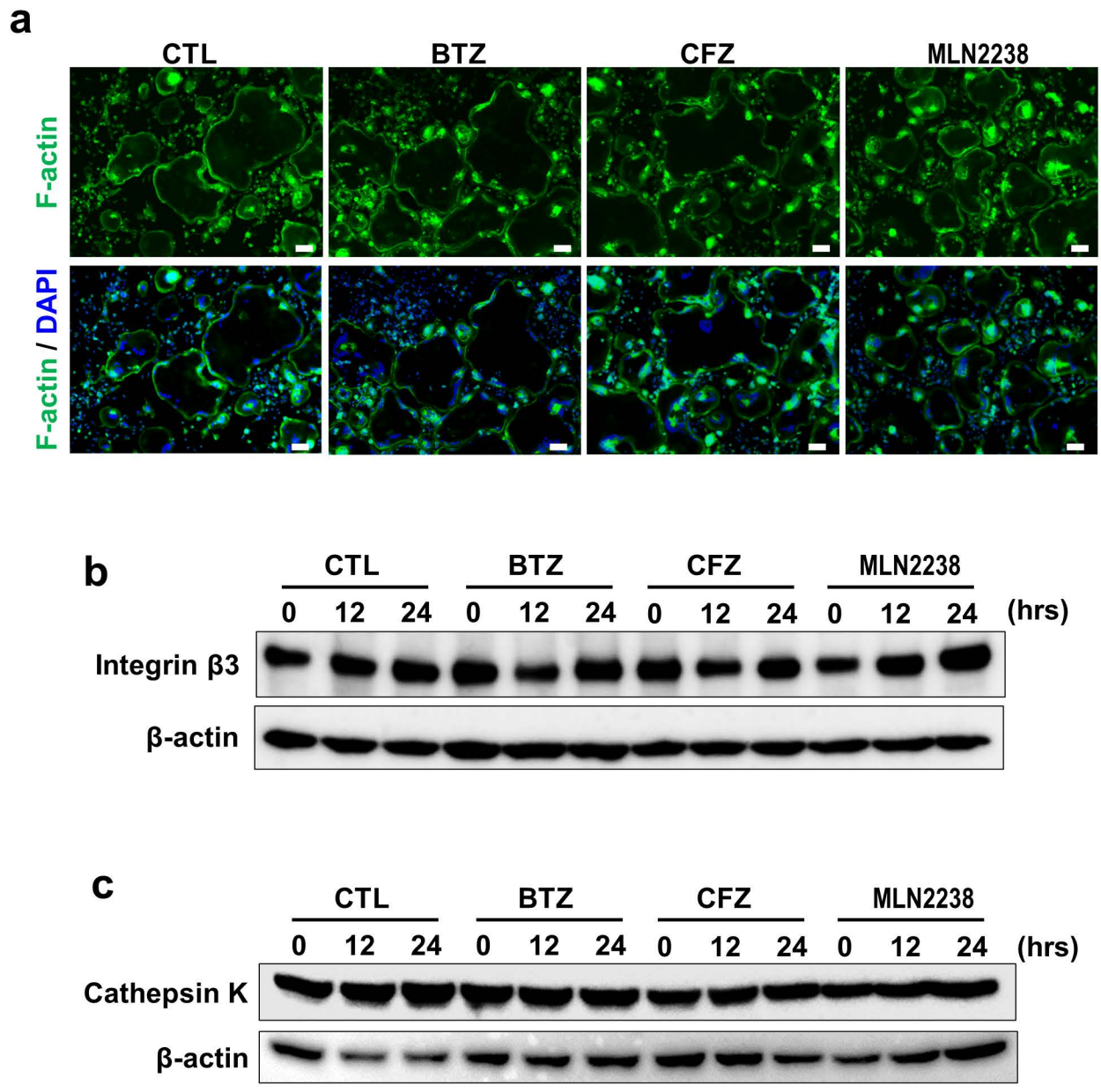
a
CTL
BTZ
CFZ
MLN2238
F-actin
F-actin / DAPI
b
CTL
BTZ
CFZ
MLN2238
0 12 24 0 12 24 0 12 24 0 12 24 (hrs)
Integrin β3
β-actin
c
CTL
BTZ
CFZ
MLN2238
0 12 24 0 12 24 0 12 24 0 12 24 (hrs)
Cathepsin K
β-actin

Figure 2

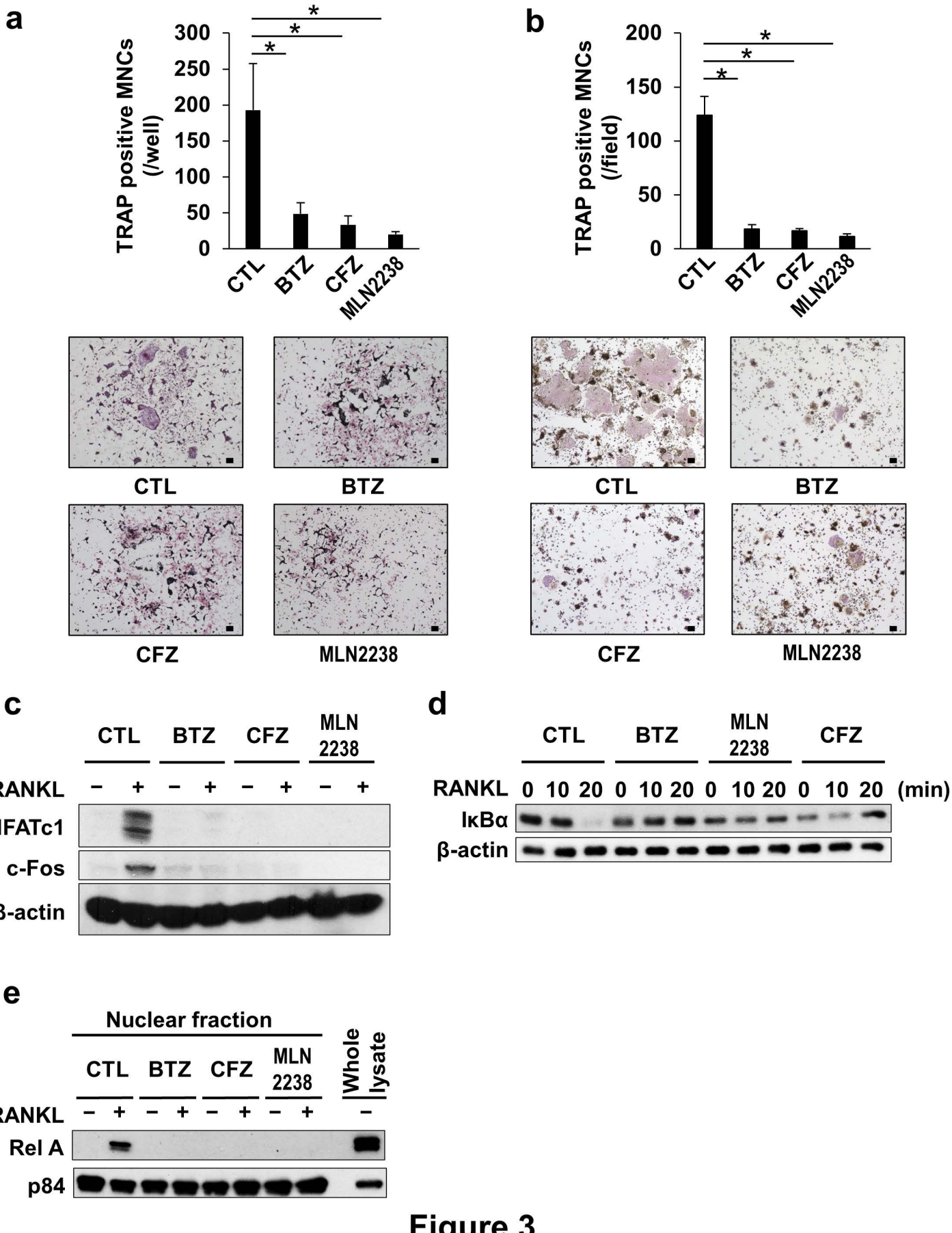
a
TRAP positive MNCs (/well)
300
250
200
150
100
50
0
*
*
*
CTL
BTZ
CFZ
MLN2238
b
TRAP positive MNCs (/field)
200
150
100
50
0
*
*
*
CTL
BTZ
CFZ
MLN2238
CTL
BTZ
CFZ
MLN2238
CTL
BTZ
CFZ
MLN2238
c
CTL
BTZ
CFZ
MLN 2238
RANKL
– + – + – + – +
NFATc1
c-Fos
β-actin
d
CTL
BTZ
MLN 2238
CFZ
RANKL
0 10 20 0 10 20 0 10 20 0 10 20 (min)
IκBα
β-actin
e
Nuclear fraction
CTL
BTZ
CFZ
MLN 2238
Whole lysate
RANKL
– + – + – + – +
–
Rel A
p84

Figure 3

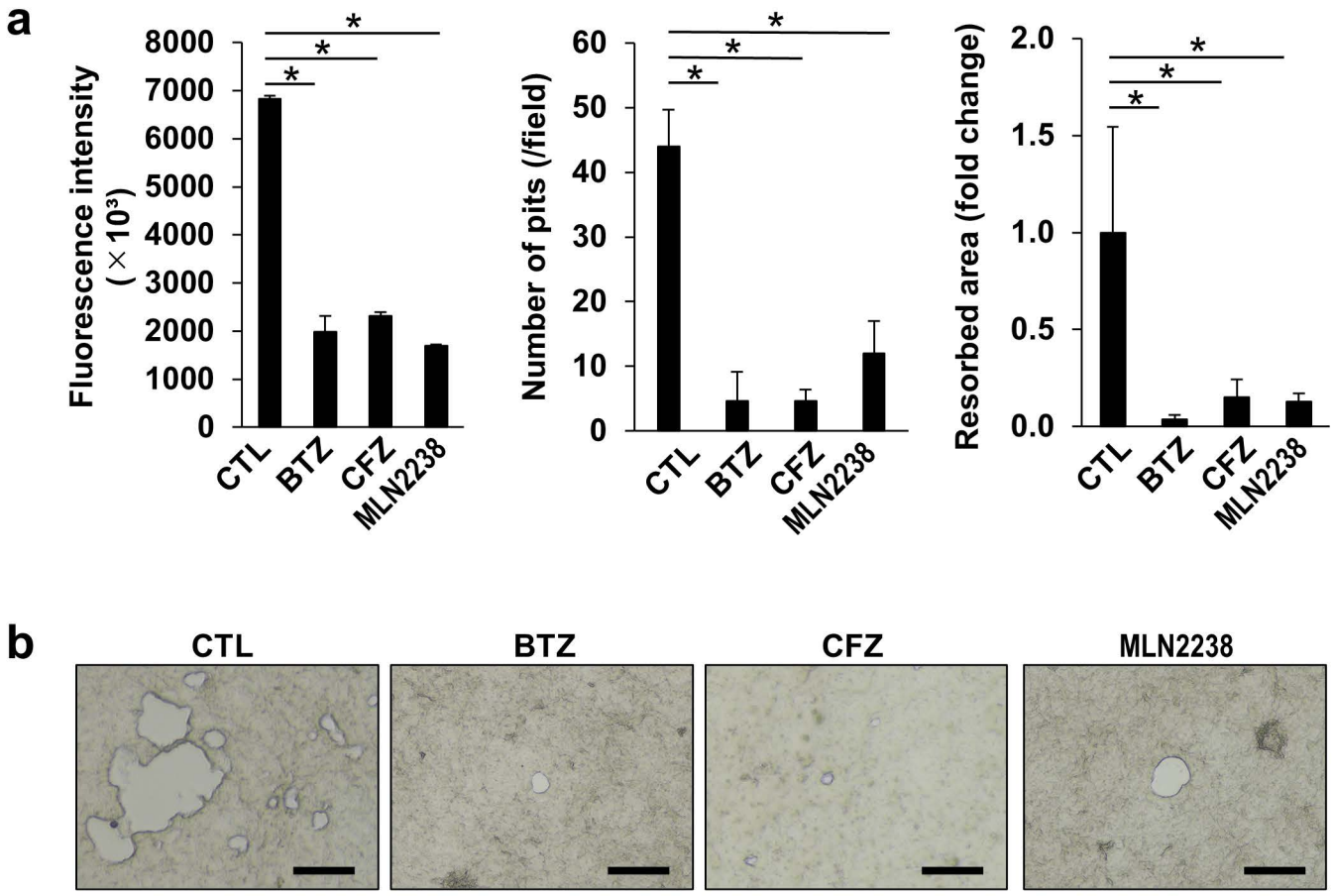
a
Fluorescence intensity (×10³)
8000
7000
6000
5000
4000
3000
2000
1000
0
CTL
BTZ
CFZ
MLN2238
Number of pits (/field)
60
50
40
30
20
10
0
Resorbed area (fold change)
2.0
1.5
1.0
0.5
0.0
b
CTL
BTZ
CFZ
MLN2238

Figure 4

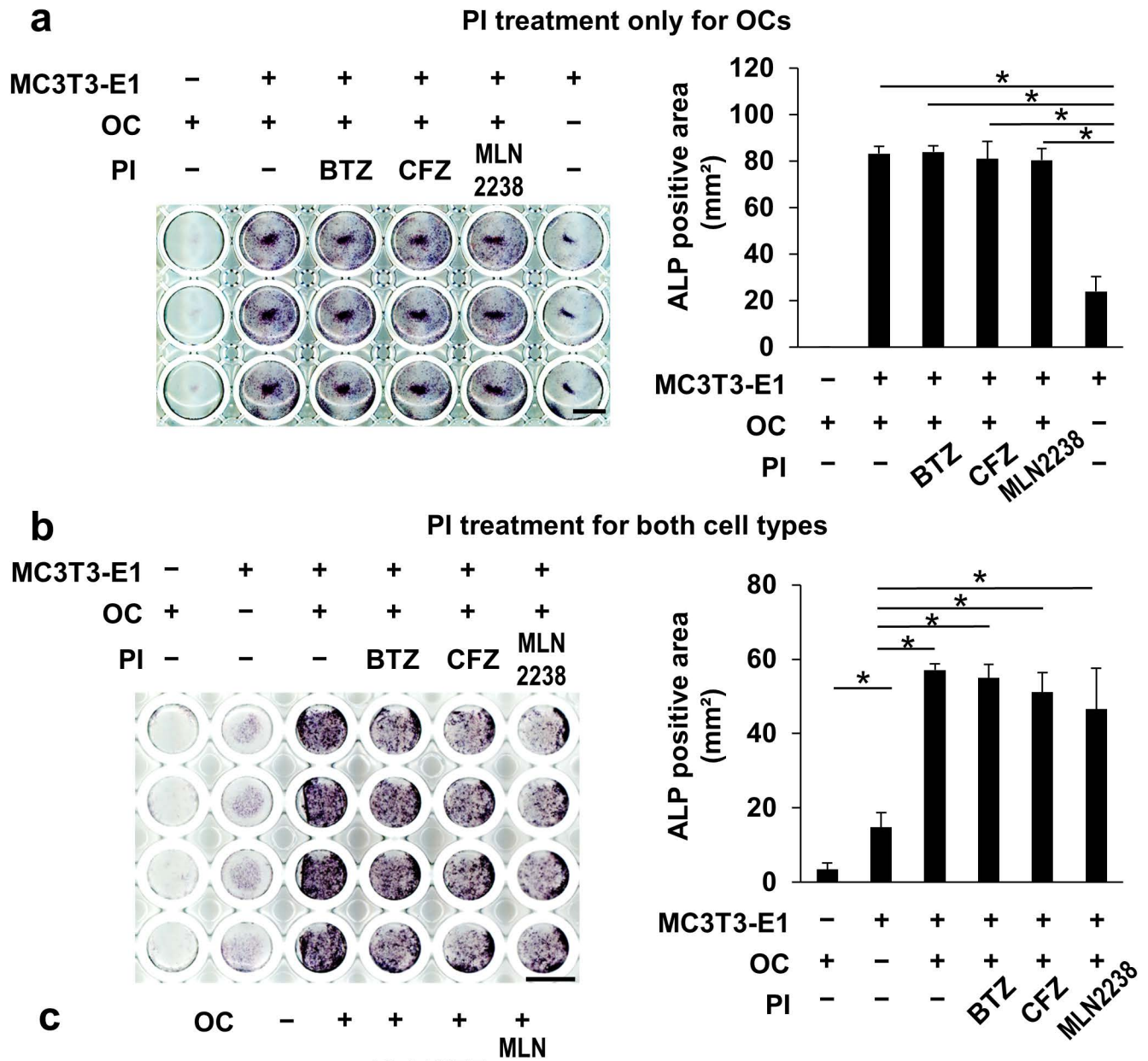
a
PI treatment only for OCs
MC3T3-E1 − + + + + +
OC + + + + + −
PI − − BTZ CFZ MLN 2238 −
ALP positive area (mm²)
120
100
80
60
40
20
0
*
*
*
*
MC3T3-E1 − + + + + +
OC + + + + + −
PI − − BTZ CFZ MLN2238 −
b
PI treatment for both cell types
MC3T3-E1 − + + + + +
OC + − + + + +
PI − − − BTZ CFZ MLN 2238
ALP positive area (mm²)
80
60
40
20
0
*
*
*
*
*
MC3T3-E1 − + + + + +
OC + − + + + +
PI − − − BTZ CFZ MLN2238
c
OC − + + + +
PI − − BTZ CFZ MLN 2238
Osterix
CDH11 (OB-cadherin)
d
CTL BTZ CFZ MLN2238
0 12 24 0 12 24 0 12 24 0 12 24 (hrs)
ephrinB2
S1P
β-actin

Figure 5